Measurement of forward η meson production with the LHCf-Arm2 detector at LHC(*)

G. Piparo([1])([2])([3]) on behalf of the LHCf Collaboration

([1]) *INFN, Sezione di Catania - Catania, Italy*
([2]) *Dipartimento di Fisica e Astronomia "Ettore Majorana", Università di Catania - Catania, Italy*
([3]) *Centro Siciliano di Fisica Nucleare e Struttura della Materia (CSFNSM) - Catania, Italy*

Summary. — In this paper, we present the data analysis strategy and the results of the forward η meson production measurement in proton-proton collisions at $\sqrt{s} = 13$ TeV, carried out with the LHCf-Arm2 detector. This is the first observation of η mesons in the forward region of proton-proton collisions at high energies and will allow a better understanding of the mechanisms by which these particles are generated. We show the comparison between the experimental data and the predictions of some hadronic interaction models that are widely used in fundamental physics. Finally, we discuss the improvements that the data collected by the LHCf experiment during Run III of the LHC will bring to this measurement.

1. – Introduction

The Large Hadron Collider forward (LHCf [1]) experiment has been specifically designed to measure the production of forward neutral particles in proton-proton and proton-Ion collisions at the Large Hadron Collider (LHC [2]), in order to provide high-energy data useful for calibrating hadronic interaction models used in simulations of the interaction between primary cosmic rays and the Earth's atmosphere. This is made possible by the performance of the experimental apparatus [3,4], consisting of two sampling calorimeters called Arm1 and Arm2, composed of two towers each and located approximately $\pm$ 140 m from interaction point 1 (IP1) of the LHC, at an angle of zero degrees to the beamline. Both detectors are made of tungsten absorbers and Gd_2SiO_5 (GSO) scintillator layers, interleaved with position-sensitive layers made of GSO bar-bundle hodoscopes for Arm1 [5] and silicon microstrip detectors for Arm2 [6]. In past years, LHCf has measured the production of neutral particles at various energies (from 0.9 to 13 TeV) in proton-proton and proton-lead collisions [7-15]. Recently, the LHCf measured the forward production of η mesons for the first time, in proton-proton collisions at $\sqrt{s} = 13$ TeV [16]. The importance of this observation is related to the role of η in hadronic interaction models. In particular, the knowledge of the forward production of η mesons at
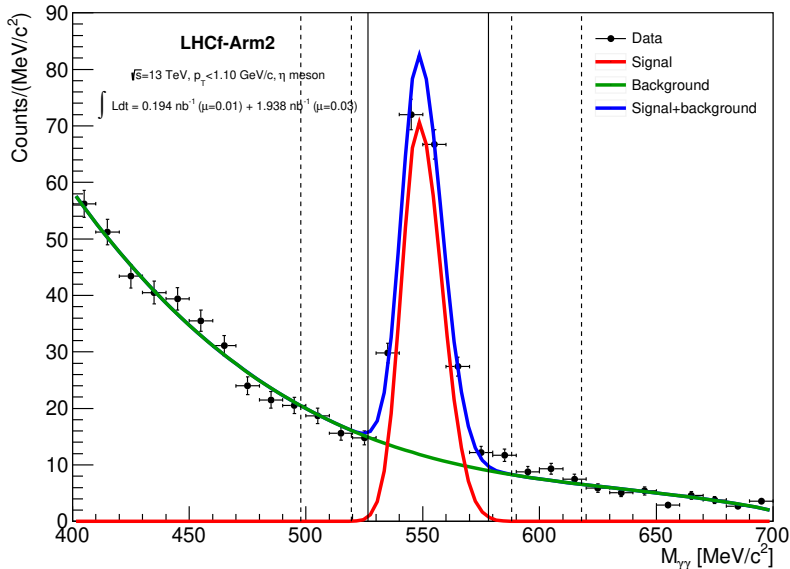

Fig. 1. – Di-photon invariant mass distribution of selected LHCf-Arm2 events with $p_T < 1.1$ GeV/c. Coloured lines indicate fit functions. Solid vertical lines border the signal window, while the dashed are the background windows. Figure from [16].

high energies, combined with that of neutral pions, allows the regulation of the parameters and mechanisms involved in the production of these two particles [17]. Furthermore, η mesons are one of the main components in the production of leptons within extended air showers produced by high-energy cosmic ray collisions with the atmosphere [18], so knowledge of their production will allow fine-tuning of models on this aspect. This paper is divided as follows: In sect. **2** we describe the strategy of analysis, performed using only the LHCf-Arm2 detector, including the event reconstruction and selection methods, the background subtraction procedure and the determination of experimental correction and uncertainties. In sect. **3** we present the measurement of the forward η production rate distribution in proton-proton collisions at $\sqrt{s} = 13$ TeV and we compare the experimental results with the prediction of four widely-used hadronic interaction models. Finally, in sect. **4** we discuss the results and future prospects of this measurement.

2. – Data analysis strategy

2′1. *Event reconstruction and selection*. – The identification of η mesons is performed by reconstructing the two photons produced in the $\eta \to \gamma\gamma$ decay (branching ratio of 39.41% [19]). Photons can hit two different towers of LHCf-Arm2 (Type I events) or both the same tower (Type II events). In this analysis only Type I η events were considered since Type II events had low statistics in our dataset. The energy and position of incident particles were reconstructed by using the calorimetric GSO layers information and the position-sensitive silicon microstrip planes transverse profile, respectively. Several selection criteria were applied:
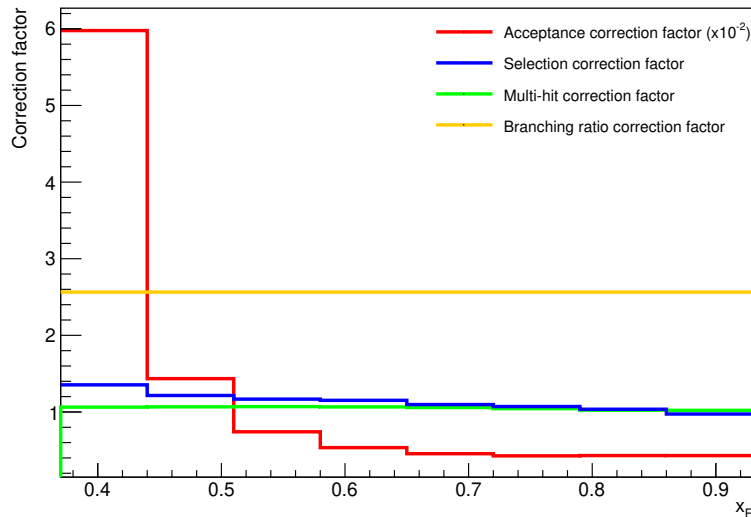
Fig. 2. – Distribution of correction factors for experimental effects in the LHCf-Arm2 detector, applied to the x_F distribution of η mesons. The acceptance correction has been scaled down by a factor of 10^{-2}. Statistical uncertainties are negligible. Figure from [16].

- *Event Type*: Only Type I events were considered due to the low acceptance of Type II events.

- *Number of hits*: Events featuring at least one background particle alongside the two photons (multi-hit events) were excluded.

- *Energy threshold*: A selection criterion was set to only include photons with energy exceeding 200 GeV to maintain about 100% trigger efficiency.

- *Position cut*: To mitigate the effects of shower leakage on energy reconstruction, only photons hitting the calorimeter within a 2 mm margin from the tower edges were considered.

- *Particle identification*: Photon and neutral hadron discrimination employed an energy-dependent threshold applied to the $L_{90\%}$ variable, which indicates the depth where 90% of the energy deposit is contained. This threshold was derived from Monte Carlo simulations with the goal of achieving 90% selection efficiency in each energy bin.

2˙2. *Background subtraction*. – η event candidates were identified by their distinctive di-photon invariant mass ($M_{\gamma\gamma}$) peak, aligning with the η meson rest mass. The η meson production spectrum was expressed as a function of the Feynman-scale variable $x_F = 2p_z/\sqrt{s}$, with p_z the z-component of the momentum and $\sqrt{s}$ the energy of the collisions in the center-of-mass reference frame. For the extraction of the x_F distribution and the subsequent background subtraction, predominantly consisting of residual hadronic
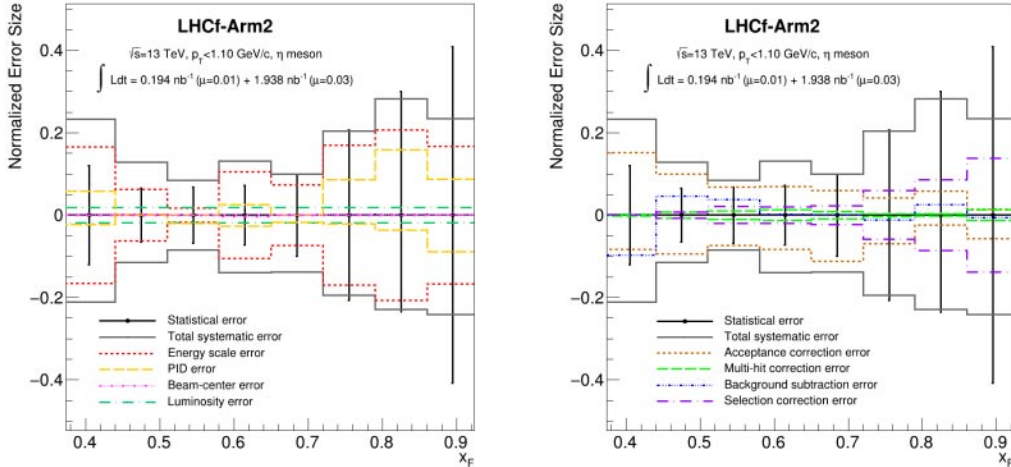
Fig. 3. – Systematic uncertainties affecting the η production measurements with the LHCf-Arm2 detector. Curves are differentiated by color-coded lines for each source, with the grey line representing the total systematic uncertainty, derived from the quadrature sum of all individual contributions. Black symbols depict statistical uncertainties. Figure from [16].

and combinatorial noise, a sideband approach was employed. Initially, a compound model function was fitted to the $M_{\gamma\gamma}$ spectrum; this function combined an asymmetric Gaussian to represent the signal with a third-degree Čebyšëv polynomial for the background. A signal window was then designated, encompassing the $M_{\gamma\gamma}$ range within three standard deviations (3σ) of the central signal peak. Additionally, two background windows were delineated in the intervals $[\pm4\sigma, \pm7\sigma]$. Following the background subtraction, approximately 1500 η candidates were identified. Figure 1 illustrates the $M_{\gamma\gamma}$ distribution, the fit functions, the signal and background regions. Due to low statistics of η mesons in our dataset, it was possible to extract the x_F distribution for only one bin of transverse momentum $p_T < 1.1$ GeV/c.

2˙3. *Estimation of experimental corrections and uncertainties*. – Several experimental corrections have been applied to the x_F spectrum of η mesons, *i.e.*, corrections for efficiency, acceptance, loss of events for multi-hit cutting and limited branching ratio. The distributions of the correction factors are shown in fig. 2. Multiple sources of systematic uncertainties were considered, primarily related to energy scale, particle identification, beam-center positioning, and luminosity measurements. Additionally, errors associated with the experimental corrections were computed. A summary of the error sources is depicted in fig. 3. A detailed description of experimental corrections and the calculation of uncertainties can be found in [16].

3. – Results of the analysis

The distribution of η production rate as a function of x_F, measured in proton-proton collisions at $\sqrt{s} = 13$ TeV by the LHCf-Arm2 for $p_T < 1.1$ GeV, is presented in fig. 4, juxtaposed with the prediction from four extensively utilized models of hadronic interactions: QGSJET II-04 [20], EPOS-LHC [21], DPMJET III-06 [22], and SIBYLL 2.3 [23].
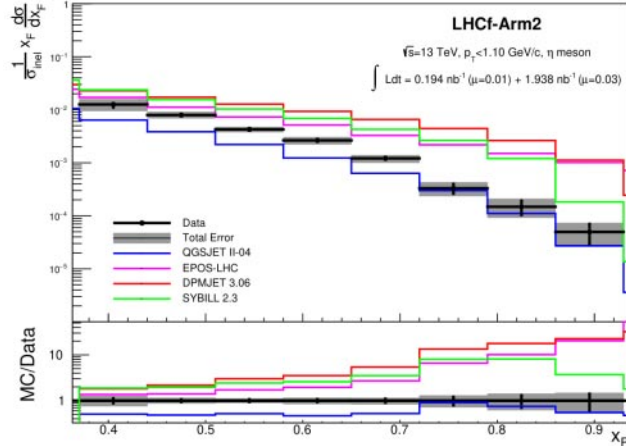
Fig. 4. – Inclusive η production rates as a function of x_F for $p_T < 1.1$ GeV/c in proton-proton collisions at a center-of-mass energy of $\sqrt{s} = 13$ TeV, measured by the LHCf-Arm2 detector. Experimental results are indicated with black markers and include statistical errors, while the grey bands represent the combined total uncertainties, which are the statistical and systematic errors added in quadrature. These results are juxtaposed with theoretical predictions at the generator level from several hadronic interaction models: QGSJET II-04 is shown with a blue line, EPOS-LHC with a magenta line, SIBYLL 2.3 with a green line, and DPMJET 3.06 with a red line. Figure from [16].

None of these models successfully match the observed distribution consistently over the full range of x_F. While QGSJETII-04 aligns well with experimental data at higher x_F values, it diverges by a factor of 2 at the lower end of the x_F spectrum.
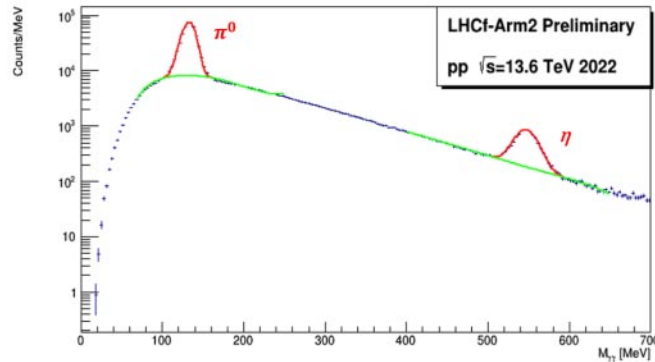

Fig. 5. – Preliminary di-photon invariant mass distribution measured by the LHCf-Arm2 detector in proton-proton collisions at $\sqrt{s} = 13.6$ TeV. The two resonance peaks refer to π^0 and η mesons, respectively.

4. – Future prospects

LHCf had a new data-taking during the RUN III of LHC, performed in September 2022, in proton-proton collisions at the record energy of $\sqrt{s} = 13.6$ TeV. Thanks to the detector read-out upgrade, we increased the statistics of η mesons by about a factor of ten. This will permit us to further investigate the η production features since thanks to the higher statistics we will improve the results presented in this paper, reducing the uncertainties on our measurements and having the possibility to extract the x_F distribution in more than one bin of p_T, which is a measurement of great importance for the fine-tuning of hadronic interaction models. Figure 5 shows the preliminary di-photon invariant mass distribution measured in proton-proton collisions at $\sqrt{s} = 13.6$ TeV by the LHCf-Arm2 detector, with a highlight on π^0 and η meson resonance peaks.

REFERENCES

[1]   LHCf COLLABORATION, *JINST*, **3** (2008) S08006.
[2]   EVANS L. and BRYANT P., *JINST*, **3** (2008) S08001.
[3]   MAKINO Y. *et al.*, *JINST*, **12** (2017) P03023.
[4]   KAWADE K. *et al.*, *JINST*, **9** (2014) P03016.
[5]   SUZUKI T. *et al.*, *JINST*, **8** (2013) T01007.
[6]   ADRIANI O. *et al.*, *JINST*, **5** (2010) P01012.
[7]   ADRIANI O. *et al.*, *Phys. Lett. B*, **715** (2012) 298.
[8]   ADRIANI O. *et al.*, *Phys. Lett. B*, **703** (2011) 128.
[9]   ADRIANI O. *et al.*, *Phys. Lett. B*, **750** (2015) 360.
[10] ADRIANI O. *et al.*, *Phys. Rev. D*, **86** (2012) 092001.
[11] ADRIANI O. *et al.*, *Phys. Rev. D*, **94** (2016) 032007.
[12] ADRIANI O. *et al.*, *Phys. Rev. C*, **89** (2014) 065209.
[13] ADRIANI O. *et al.*, *Phys. Lett. B*, **780** (2018) 233.
[14] ADRIANI O. *et al.*, *J. High Energy Phys.*, **2018** (2018) 73.
[15] ADRIANI O. *et al.*, *J. High Energy Phys.*, **2020** (2020) 16.
[16] ADRIANI O. *et al.*, *J. High Energy Phys.*, **2023** (2023) 169.
[17] RIEHN F. *et al.*, *Phys. Rev. D*, **102** (2020) 063002.
[18] FEDYNITCH A. *et al.*, *Phys. Rev. D*, **100** (2019) 103018.
[19] WORKMAN R. L. *et al.*, *Prog. Theor. Exp. Phys.*, **2022** (2022) 083C01.
[20] OSTAPCHENKO S., *Phys. Rev. D*, **83** (2011) 014018.
[21] PIEROG T. *et al.*, *Phys. Rev. C*, **92** (2015) 034906.
[22] BOPP F. W. *et al.*, *Phys. Rev. C*, **77** (2008) 014904.
[23] RIEHN F. *et al.*, in *Proceedings of the ICRC2015 International Cosmic Ray Conference, The Hague (Netherlands), 30 July-6 August 2015*, Vol. **238** (PoS ICRC2015) 2016.